PRAMANA
— journal of
physics

Vol. 72, No. 4
April 2009
pp. 689–707

Neutron and proton shell closure in the superheavy region via cluster radioactivity in $^{280-314}116$ isotopes

K P SANTHOSH* and R K BIJU
P.G. Department of Physics & Research Centre, Payyanur College, Payyanur 670 327, India
*Corresponding author. E-mail: kpsanthosh@eth.net; drkpsanthosh@gmail.com

MS received 15 October 2008; revised 8 December 2008; accepted 23 December 2008

Abstract. Based on the concept of cold valley in fission and fusion, the radioactive decay of superheavy$^{280-314}116$ nuclei was studied taking Coulomb and proximity potentials as the interacting barrier. It is found that the inclusion of proximity potential does not change the position of minima but minima become deeper which agrees with the earlier findings of Gupta and co-workers. In addition to alpha particle minima, the other deepest minima occur for ^{8}Be, ^{12,14}C clusters. In the fission region two deep regions are found each consisting of several comparable minima, the first region centred on ^{208}Pb and the second is around ^{132}Sn. The cluster decay half-lives and other characteristics are computed for various clusters ranging from alpha particle to ^{70}Ni. The computed half-lives for alpha decay match with the experimental values and with the values calculated using Viola–Seaborg–Sobiczewski (VSS) systematic. The plots connecting computed Q values and half-lives against neutron number of daughter nuclei were studied for different clusters and it is found that the next neutron shell closures occur at $N = 162, 172$ and 184. Isotopic and isobaric mass parabolas are studied for various cluster emissions and minima of parabola indicate neutron shell closure at $N = 162$, 184 and proton shell closure at $Z = 114$. Our study shows that $^{276}_{162}114$ is the deformed doubly magic and $^{298}_{184}114$ is the spherical doubly magic nuclei.

Keywords. Cluster decay; alpha decay.

PACS Nos 23.60.+e; 23.70.+j; 27.90.+b

1. Introduction

The radioactive decay of nuclei emitting particle heavier than alpha particle termed as cluster radioactivity was first predicted by Sandulescu *et al* [1] in 1980 on the basis of quantum mechanical fragmentation theory [2]. This rare, cold (neutronless) process is intermediate between alpha decay and spontaneous fission. The rare nature of this process is due to the fact that cluster emission is marked by several alpha emissions. Experimentally, Rose and Jones [3] first observed such decay in

1984 in the radioactive decay of ^{223}Ra by the emission of ^{14}C. At present about 20 parent nuclei from ^{221}Fr to ^{242}Cm emitting clusters ranging from ^{14}C to ^{34}Si are confirmed [4].

The exploration of cluster radioactivity in the superheavy island did not receive much attention because of the instability of nuclei in this region. From theoretical point of view, the extension of the periodic table towards the superheavy 'island of stability' is very important for testing and developing nuclear structure models. The half-lives of different radioactive decay models such as alpha decay, cluster radioactivity and fission are important to identify the decay chains of superheavy elements, which are the experimental signatures of their formation in fusion reaction.

In the present work an attempt is made to examine the possibility of cluster emission from nuclei in the superheavy region with an aim to find the next neutron and proton shell closure in this region. Based on the concept of cold valleys, Kumar *et al* [5] studied cluster emission from the superheavy nucleus ^{277}Ds and from its alpha decay products ^{273}Hs and ^{269}Sg. They conclude that in addition to alpha decay and fission ^{14}C, ^{34}Si and ^{50}Ca are the optimal cases of cluster radioactivity, but the predicted half-lives for these clusters are of huge order of magnitude than the expected compound nucleus lifetime. Singh *et al* [6] have proposed a theoretical approach to study the cluster decay of some heavy and superheavy nuclei [7,8]. Their model is based on fragmentation theory [9] and on the preformed cluster decay model proposed by Malik *et al* [10]. Nuclear lifetimes for cluster radioactivity of superheavy elements and nuclei far off the beta-stability line (Z = 52–122) have been calculated in a pioneering work by Poenaru *et al* [11].

In the 1960s a number of theoretical predictions [12] were made that pointed towards the existence of an island of long-lived superheavy elements centred on $Z = 126$, $N = 184$. One of the fundamental factors in the study of superheavy elements is the prediction and/or production of doubly magic nucleus, next to $Z = 82$, $N = 126$ (^{208}Pb). The existence of superheavy nuclei with $Z \geq 104$ is due to quantum shell effects, and pronounced shell gaps can stabilize nuclei. In the superheavy mass region, the proton numbers $Z = 114, 120, 126$ and neutron numbers $N = 172$, 184 have been predicted to be magic numbers. Recently, the density distributions of superheavy nuclei have become interesting for the structure study of the heaviest nuclei [13–16]. Later, Patra *et al* [17] predicted $Z = 120$ and $N = 172$ or 184 as the next possible magic numbers using axially deformed relativistic mean field calculations.

The superheavy elements are produced by complete fusion between an incident ion and a target ion. Discovery of 'superheavy' elements has been announced at the Lawrence Berkeley National Laboratory. One of the experiments done at Dubna [18] was designed to investigate the radioactive properties of the isotopes of element 116, the α-decay daughters of $Z = 118$ isotopes produced in the reaction ^{249}Cf + ^{48}Ca. In this reaction two new isotopes of element 116 have been synthesized and they undergo sequential α decays terminated by spontaneous fission. ^{290,292,293}116 have been produced at higher excitation energies and different cross-sections [19]. The isotope of ^{292}116 was identified in the reaction of curium with calcium (^{248}Cm + ^{48}Ca $\rightarrow$ ^{292}116 + 4_0n^1).

Within Coulomb and proximity potential model [20–23] we have studied cluster emission from various proton-rich nuclei with $Z = 54$–64 and $N = 54$–72 leading to ^{100}Sn daughter. We have also studied the cold valleys in the radioactive decay of $^{248-254}$Cf isotopes [24] and the computed alpha decay half-life values are in close agreement with the experimental data. Recently, we have proposed a semi-empirical model [25] for determining the half-lives of radioactive nuclei exhibiting cluster radioactivity. The semi-empirical formula is applied to alpha decay of parents with $Z = 85$–102 and is compared with experimental data. In this paper we extend our studies to superheavy isotopes $^{280-314}116$ emitting clusters ranging from alpha particle to ^{70}Ni using the Coulomb and proximity potential model. The details of the model are given in §2 and results, discussion and conclusion are given in §3.

2. The model

The interacting potential barrier for a parent nucleus exhibiting exotic decay is given by

$$V = \frac{Z_1 Z_2 e^2}{r} + V_{\rm p}(z) + \frac{\hbar^2 \ell(\ell+1)}{2\mu r^2}, \quad \text{for} \quad z > 0. \tag{1}$$

Here Z_1 and Z_2 are the atomic numbers of daughter and emitted cluster, r is the distance between fragment centres, ℓ is the angular momentum, μ is the reduced mass and $V_{\rm p}$ is the proximity potential given by Blocki *et al* [26]

$$V_{\rm p}(z) = 4\pi\gamma b \left[\frac{C_1 C_2}{(C_1 + C_2)}\right] \Phi\left(\frac{z}{b}\right). \tag{2}$$

With the nuclear surface tension coefficient,

$$\gamma = 0.9517[1 - 1.7826(N-Z)^2/A^2] \ \text{MeV/fm}^2, \tag{3}$$

where N, Z and A represent neutron, proton and mass number of the parent. The universal proximity potential, Φ is given as [27]

$$\Phi(\varepsilon) = -4.41 \mathrm{e}^{-\varepsilon/0.7176}, \quad \text{for } \varepsilon \geq 1.9475 \tag{4}$$

$$\Phi(\varepsilon) = -1.7817 + 0.9270\varepsilon + 0.0169\varepsilon^2 - 0.05148\varepsilon^3, \quad \text{for } 0 \leq \varepsilon \leq 1.9475. \tag{5}$$

With $\varepsilon = z/b$, where the width (diffuseness) of the nuclear surface $b \approx 1$ and Siissmann central radii C_i of fragments related to sharp radii R_i is

$$C_i = R_i - \left(\frac{b^2}{R_i}\right). \tag{6}$$

For R_i we use semi-empirical formula in terms of mass number A_i as [26]

$$R_i = 1.28A_i^{1/3} - 0.76 + 0.8A_i^{-1/3}. \tag{7}$$

Using one-dimensional WKB approximation, the barrier penetrability P is given as

$$P = \exp\left\{-\frac{2}{\hbar}\int_a^b \sqrt{2\mu(V-Q)}\mathrm{d}z\right\}. \tag{8}$$

Here the mass parameter is replaced by $\mu = mA_1A_2/A$, where m is the nucleon mass and A_1, A_2 are the mass numbers of the daughter and emitted cluster respectively. The turning points a and b are determined from the equation $V(a) = V(b) = Q$. The above integral can be evaluated numerically or analytically, and the half-life is given by

$$T_{1/2} = \left(\frac{\ln 2}{\lambda}\right) = \left(\frac{\ln 2}{\nu P}\right), \tag{9}$$

where $\nu = (\omega/2\pi) = (2E_\mathrm{v}/h)$ represents the number of assaults on the barrier per second and λ is the decay constant. E_v, the empirical zero point vibration energy, is given as [28]

$$E_\mathrm{v} = Q\left\{0.056 + 0.039\exp\left[\frac{(4-A_2)}{2.5}\right]\right\}, \quad \text{for } A_2 \geq 4. \tag{10}$$

3. Results, discussion and conclusion

We studied the cluster radioactivity based on the potential barrier determined by two-sphere approximation, as the sum of Coulomb and nuclear proximity potentials [29] for the touching and separated configuration ($z > 0$). Here z is the distance between the near surfaces of the fragments. The possibility to have a cluster decay process is,

$$Q = M(A,Z) - M(A_1,Z_2) - M(A_2,Z_2) > 0, \tag{11}$$

where $M(A,Z)$, $M(A_1,Z_1)$, $M(A_2,Z_2)$ are the atomic masses of the parent, daughter and cluster respectively.

The concept of cold valley was introduced in relation to the structure of minima in the so-called driving potential, which is defined as the difference between the interaction potential and the decay energy (Q-value) of the reaction. Q-values are computed using experimental binding energies of Audi and Wapstra [30] and some values are taken from finite-range droplet model tables. The interaction potential is a function of distance of separation of interacting fragments. The driving potential of the compound nucleus is calculated for all possible cluster–daughter combinations as a function of mass and charge asymmetries, $\eta = (A_1 - A_2)/(A_1 + A_2)$ and $\eta_Z = (Z_1 - Z_2)/(Z_1 + Z_2)$ for the touching configuration of the fragments. That is, the distance between the fragments $r = C_1 + C_2$, where C_1 and C_2 are the Siissmann central radii. The charges of the fragments are fixed by minimizing the

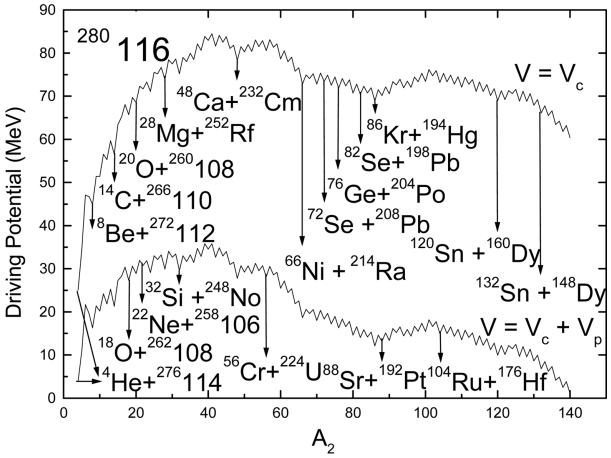

Figure 1. The plot of driving potential vs. A_2, the mass of one fragment for $^{280}116$ isotope. The calculations are made for touching configuration, $r = C_1 + C_2$.

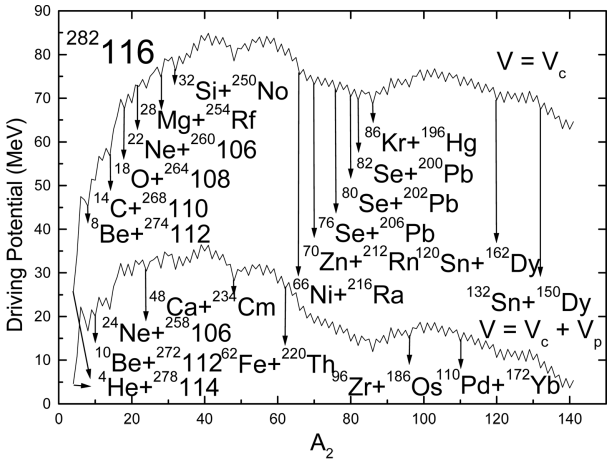

Figure 2. The plot of driving potential vs. A_2 the mass of one fragment for $^{282}116$ isotope. The calculations are made for touching configuration, $r = C_1 + C_2$.

driving potential for fixed η and r. In the charge asymmetric coordinate η_z, for every fixed mass pair (A_1, A_2) a single pair of charges is determined among all possible combinations. Figures 1 and 2 represent the plots of driving potential vs. mass A_2 of one fragment for the isotopes $^{280}116$ and $^{282}116$ with and without including proximity potential. The occurrence of the mass-asymmetry valleys in these figures is due to the shell effects of one or both fragments. The inclusion of the proximity potential does not change the position of the minima but they become deeper. This result is now known for more than two decades, first shown by Saroha *et al* [31]. The minima in potential energy curve represent the most probable decay.

In figures 1 and 2 it can be seen that in addition to alpha particle, ^{8}Be, ^{12,14}C, ^{18,20}O, ^{32,34}Si, ^{28}Mg, ^{32,34}Si, ^{48,50}Ca clusters are probable for emission from $^{280-282}$116. Moving to the fission region there are two deep regions each consisting of several comparable minima, the first region centred on ^{208}Pb and second is around ^{132}Sn. From the cold valley approach the first minimum is at ^{72}Se+^{208}Pb due to the double magicity of ^{208}Pb ($Z = 82$, $N = 126$). Another minimum is occurring due to the magic neutron shell $N = 126$ of ^{214}Ra, i.e. at ^{214}Ra+^{66}Ni while the other splittings ^{64}Ni+^{216}Ra, ^{70}Zn+^{210}Rn and ^{74}Ge+^{206}Po are due to the presence of near magic neutron shell closures ($N \approx 126$). In the case of the second region, the first minimum is at ^{132}Sn+^{148}Dy due to the double magicity of ^{132}Sn ($Z = 50$ and $N = 82$) while other splittings are at ^{128}Te+^{152}Gd and ^{130}Xe+^{150}Sm.

It is evident from the minima (cold valley) that in addition to alpha particle, ^{8}Be, ^{14}C, ^{20}O, ^{34}Si, ^{28}Mg, ^{32,34}Si, ^{48,50}Ca are the most probable cases of cluster emission from $^{284-314}$116 isotopes. In the fission region, these curves show two deep minima, same as in figures 1 and 2. One of them is 'lead valley' and other is the 'Sn valley'. In lead valley, some other valleys are situated near to it. These valleys show the magicity of neutron number $N = 126$. Examples are ^{68}Ni+^{214}Ra and ^{74}Se+^{208}Pb in ^{282}116, ^{76}Se+^{208}Pb in ^{284}116, ^{72}Ni+^{214}Ra, ^{78}Se+^{208}Pb in ^{286}116, ^{80}Se+^{208}Pb in ^{288}116, ^{82}Se+^{208}Pb in ^{290}116, ^{84}Se+^{208}Pb in ^{292}116, ^{86}Se+^{208}Pb in ^{294}116 and ^{88}Se+^{208}Pb and ^{90}Kr+^{206}Hg in ^{296}116 etc. Finally in the second region the cold valleys (Sn valley) are situated at ^{120}Sn+^{162}Dy in ^{282}116, ^{126}Sn+^{162}Dy in ^{288}116, ^{134}Te+^{158}Gd in ^{292}116 and ^{130}Sn+^{166}Dy, ^{132}Sn+^{164}Dy and ^{134}Te+^{162}Gd etc.

The angular momentum ℓ carried away in the cluster decay process, appearing in eq. (1) is very small ($\approx 5\hbar$) and its contribution to half-life is shown to be small [23,28] which is decided by the spin parity conservation. In the present work, calculations are done assuming zero angular momentum transfers. The proximity potential was first used by Shi and Swiatecki [32] in an empirical manner and has been quiet extensively used over a decade by Malik and Gupta [33] in the preformed cluster model (PCM) which is based on the pocket formula of Blocki *et al* [26] which is given as

$$\Phi(\varepsilon) = -\left(\frac{1}{2}\right)(\varepsilon - 2.54)^2 - 0.0852(\varepsilon - 2.54)^3, \quad \text{for } \varepsilon \leq 1.2511 \tag{12}$$

$$\Phi(\varepsilon) = -3.437 \exp\left(\frac{-\varepsilon}{0.75}\right), \quad \text{for } \varepsilon \geq 1.2511. \tag{13}$$

In the present model, another formulation of proximity potential [27] as given in eqs (4) and (5) have been used. Inclusion of proximity potential reduces height of the barrier which closely agrees with the experiment. In the present model cluster formation of probability is taken as unity for all clusters irrespective of their masses. So the present model differs from the preformed cluster model by a factor P_0, the cluster formation of probability. In the present model assault frequency ν is calculated for each parent–cluster combination which is associated with zero point vibration energy but Shi and Swiatecki [32] get ν empirically, unrealistic values 10^{22} for even A parent and 10^{20} for odd A parent.

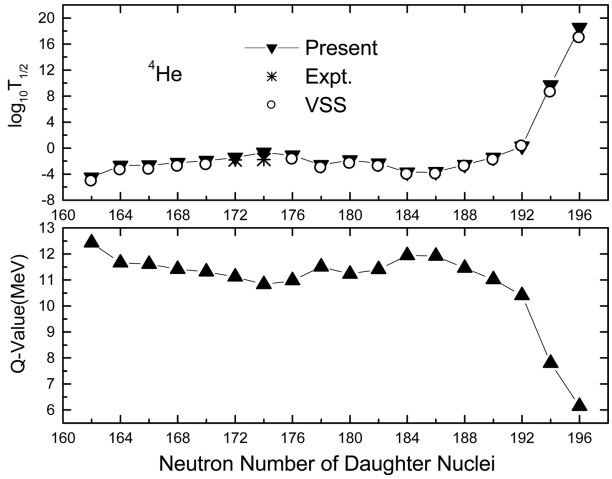

Figure 3. Computed Q-value and half-life vs. neutron number of daughter nuclei with $Z = 116$ emitting from alpha decay. Computed half-life values are compared with experimental and VSS values.

Figures 3–6 are the plots of computed half-lives and Q-values for clusters like ^{4}He, ^{10}Be, ^{14,16}C and ^{16,18}O against the neutron number of the daughter. It is found that these figures are mirror reflections of the other. In half-live plots, at the points $N = 162$, 172 and 184 a dip is present and in plot for Q-value a rise is present at $N = 162$, 172 and 184. Both these facts show that these are due to the presence of sub-magic shell closure at 162 and spherical neutron shell closure at 172 and 184. From RMF [34] formalism, neutron number $N = 162$ has been predicted to exhibit shell closure. Cwiok *et al* [35] predicted that $N = 162$ for $Z =$ 108–110 indicate the bunching of levels with spin and particles $1/2^+$, $3/2^+$, $7/2^+$, $9/2^+$ and $11/2^-$ and also the large gap of about 1 MeV up to the next higher level. Gambhir *et al* [36] showed that the isotopes of $Z = 116$ turn out to be spherical or nearly spherical, in the neighbourhood of neutron number 172 (^{288}116). This fact supports the conclusion that spherical shell closure occurs at neutron number 172 and from relativistic mean field method, Rutz *et al* [37] predicted $N = 172$ as the next possible spherical magic shell closure.

Figure 3 represents the plot of computed half-lives and Q-values for alpha decay against neutron number of the daughter nuclei. The computed alpha decay half-lives for ^{290}116 (Present $= -1.443$, Expt. $= -1.82$ [38]), ^{292}116 (Present $= -0.68$, Expt. $= -1.74$ [39]) isotopes match with the experimental values within one order of magnitude and also with the values calculated using the Viola–Seaborg semi-empirical relationship with constants determined by Sobiczewski *et al* [40] is given by

$$\log_{10} T_{1/2} = [aZ + b][Q/\mathrm{MeV}]^{-1/2} + cZ + d + h_{\log}, \tag{14}$$

where the half-life is in seconds, the Q-value is in MeV and Z is the atomic number of parent nucleus. Instead of using original set of constants by Viola and Seaborg, more recent values

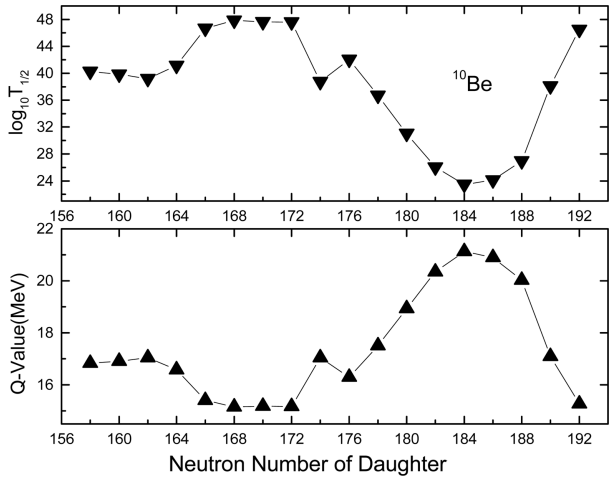

Figure 4. Computed Q-value and half-life vs. neutron number of daughter nuclei with $Z = 116$ emitting from ^{10}Be isotope.

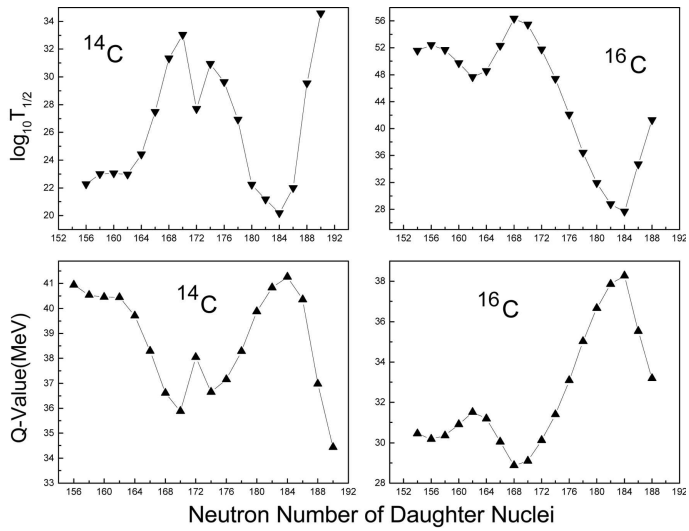

Figure 5. Computed Q-value and half-life vs. neutron number of daughter nuclei with $Z = 116$ emitting from ^{14,16}C isotopes.

$$a = +1.66175, \quad b = -8.5166, \quad c = -0.20228, \quad d = -33.9069 \qquad (15)$$

that were determined in an adjustment taking account of new data for new even–even nuclei [40] are used. The quantity $h_{\log}$ in eq. (14) accounts for the hindrances associated with odd proton and odd neutron numbers given by Viola–Seaborg [41], namely

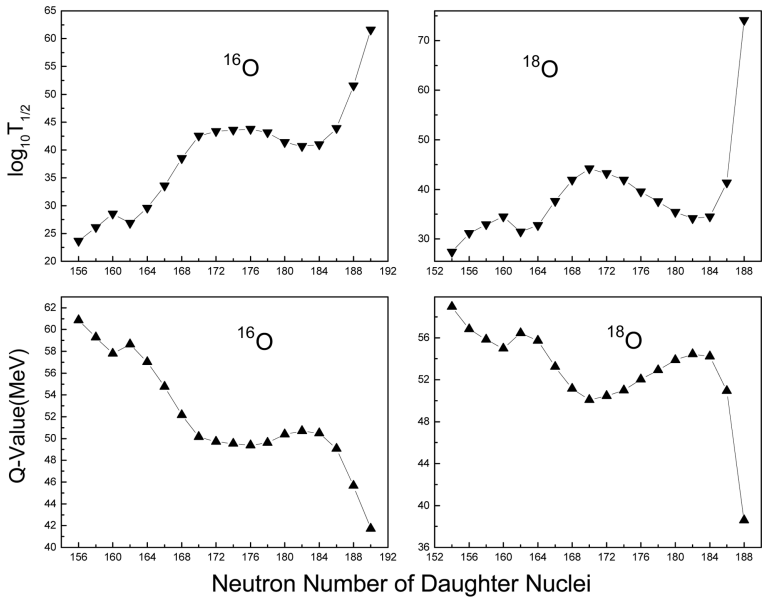

Figure 6. Computed Q-value and half-life vs. neutron number of daughter nuclei with $Z = 116$ emitting from ^{16,18}O isotopes.

$$\begin{aligned} h_{\log} &= 0, \text{ for } Z \text{ even, } N \text{ even,} \\ h_{\log} &= 0.772, \text{ for } Z \text{ odd, } N \text{ even,} \\ h_{\log} &= 1.066, \text{ for } Z \text{ even, } N \text{ odd,} \\ h_{\log} &= 1.114, \text{ for } Z \text{ odd, } N \text{ odd.} \end{aligned} \tag{16}$$

We see that the computed alpha half-lives closely agree with VSS alpha half-life.

Figure 4 represents the plot of computed half-lives and Q-values for ^{10}Be decay against neutron number of the daughter nuclei. In half-life plots, at the point $N = 174$, a dip is present and in plot for Q-value a rise is present at $N = 174$. This shows a neutron shell closure at $N = 174$. We would like to point out that SHF+ Sly4 [35] results show a pronounced shell effect for ^{289}116 which is related to the deformed shells at $Z = 116$ and $N = 174$. The NL-Z2 also predicts a deformed $N = 174$ as well but a deformed $Z = 114$ proton shell (see figure 2 of [42]) that leads to a broad plateau at smaller atomic numbers.

According to eqs (8) and (9) it is obvious that peak in Q-value appears as a dip in half-lives or vice versa. The Q-values in the plots (figures 3–6) are the Q-values corresponding to the driving potential minima of each mass asymmetric combination. Half-lives are calculated for these Q-values for which the driving potential is minimum. For a particular mass asymmetric combination, a pair of charges is singled out for which the driving potential is minimum. The Q-value corresponding to the driving potential minimum need not necessarily be the maximum Q-value for that particular mass asymmetry. In the case of ^{280}116 parent ten clusters with different Z values and with the same $A_2 = 34$ are possible for emission with Q-values varying from 39.54 MeV (for ^{34}Na) to 135.56 MeV (for ^{34}S), but the minimum

driving potential is obtained for ^{34}Si cluster (Q = 115.747 MeV) not for ^{34}S for which Q-value is maximum. In the case of $A_2 = 16$, we have shown Q-value plot for ^{16}C and ^{16}O because in some parents ^{16}O is in the cold valley (for e.g. in ^{280}116) and in some parents ^{16}C is in the cold valley (for e.g. in ^{284}116, ^{286}116).

Cluster radioactivity is energetically possible only if Q-value is positive. If we plot all positive Q-values (or half-lives) against A_2, the mass of light fragment, the plot will not give any information on magic shell closure even though information on shell effects are contained in the Q-value. We took those Q-values (or half-lives) which lie in the cold valley, i.e. the proper choice of Q-value (or half-lives) will give information about magicity (figures 3–6). The dynamical quantity, the half-life, in principle depends not only on nuclear structure but also on nuclear inertia. The computation of half-life is to find the stability of $^{280-314}$116 parent nuclei against cluster emission. In cluster radioactivity half-lives up to 10^{30} s is probable for emission. The parent nuclei with $T_{1/2} > 10^{30}$ s are stable against cluster decay.

The present calculations have been done to find the alpha decay half-lives and to determine the most probable heavy cluster emissions. Our calculated alpha half-life values for ^{290,292}116 isotopes agree well with experimental values. Therefore, we presume that the present alpha half-lives of other isotopes will be a guide to future experiments.

Poenaru *et al* studied the plot connecting Q-value and $\log_{10} T_{1/2}$ against neutron number (figure 2 of ref. [43]). The peak in Q-value corresponds to a dip in $\log_{10} T_{1/2}$ which is attributed to neutron shell closures at 126, 152 and 162 for alpha decay of parent with Z ranging from 96 to 117. These authors have done a similar work (figures 3 and 4 of ref. [44]) in which they show the proton shell closure of $Z = 82$ and neutron shell closure of $N = 126$ for parents decaying to daughters with atomic numbers ranging from 80 to 84. Zhang *et al* using GLDM, studied the plot connecting Q-value and logarithmic half-life against neutron number of parent with $Z = 106$–120 decaying by alpha emission. Both plots are found to be perfect inverse reflection of the other (figure 1 of ref. [45]) and shows the sub-magic shell closure at $N = 162$ and spherical shell closure at $N = 184$. Similar plots connecting Q-value and $\log_{10} T_{1/2}$ against neutron number of daughter for various bismuth isotopes in the range $187 \leq A \leq 214$ (figure 4 of ref. [46]) was studied by Tavares *et al* and they found a peak in Q-value corresponding to a dip in $\log_{10} T_{1/2}$, which indicates the neutron shell closure at $N = 126$.

Figures 7 and 8 represent the computed half-life vs. mass number of parent nuclei emitting various clusters ranging from ^{8}Be to ^{70}Ni. From these plots it is clear that in addition to alpha particle ^{8}Be, ^{12}C and ^{14}C clusters are most probable for the emission with half-life, $T_{1/2} < 10^{30}$ s.

Mass parabola (plot connecting $-\Delta M$, the difference in masses of parent and daughter nuclei vs. neutron number of daughter nuclei) for various clusters emitted from various $Z = 116$ parents is studied. Figure 9 represents isotopic mass parabola for ^{16}C, ^{20}O, ^{10}Be, ^{14}C cluster emissions from various $Z = 116$ parents. Minima (slope discontinuity) of mass parabola occur at magic neutron number $N = 162$, 184. We would like to mention that minima of mass parabola represent the lowest half-life $T_{1/2}$ for the corresponding cluster. Half-life measurement for cluster emission may not be possible because few atoms of short-lived superheavy nuclei are produced but in future more mass measurements will be available and by not-

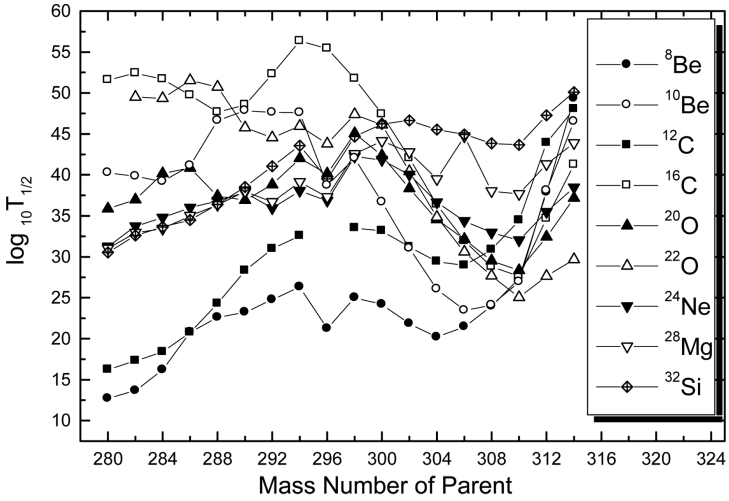

Figure 7. Computed half-life vs. mass number of parent nuclei with $Z = 116$ emitting various clusters ranging from ^{8}Be to ^{32}Si.

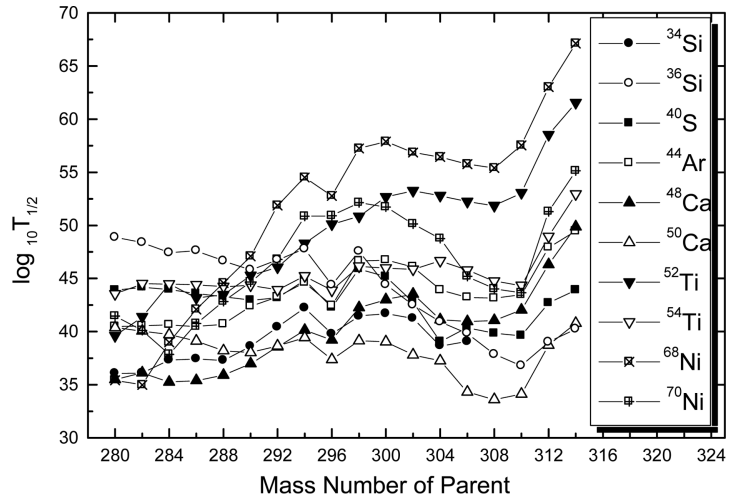

Figure 8. Computed half-life vs. mass number of parent nuclei with $Z = 116$ emitting various clusters ranging from ^{34}Si to ^{70}Ni.

ing the minima in mass difference, it will be possible to find neutron magicity in superheavy region.

Tables 1 and 2 show the computed half-life values and other characteristics of $^{280-314}116$ isotopes decaying by the emission of the most probable clusters. It is clear that ^{8}Be from $^{304}116$, ^{14}C is from $^{308}116$ and ^{22}O from $^{314}116$ isotopes are the most probable. All these decay show the role of spherical shell closure of daughter at $N = 184$. ^{8}Be cluster from $^{302}116$, ^{10}Be and ^{12}C from $^{304}116$, ^{8}Be, ^{10}Be, ^{12}C and ^{14}C from $^{306}116$, ^{10}Be, ^{12,16}C from $^{308}116$, ^{14}C, ^{16}C and ^{20}O from $^{310}116$ and

Table 1. The computed half-life values, barrier penetrability and other characteristics of $^{280-292}116$ isotopes with zero angular momentum transfers. Masses are taken from [30,51].

Parent nuclei	Emitted cluster	Daughter nuclei	Q-value (MeV)	Penetrability P	Decay constant	$\log_{10} T_{1/2}$
$^{280}116$	^{4}He	$^{276}114$	12.43	3.838e−19	2.191e+04	−4.50
			12.97[a]	5.702e−16	3.397e+05	−5.60
	^{8}Be	$^{272}112$	24.67	1.849e−34	1.407e−13	12.69
			25.36[a]	5.991e−33	4.693e−12	11.17
	^{12}C	$^{268}110$	43.64	3.311e−38	4.024e−17	16.24
			44.64[a]	1.759e−36	2.188e−15	14.51
$^{282}116$	^{4}He	$^{278}114$	11.66	6.514e−19	3.488e+02	−2.71
			12.44[a]	4.385e−17	2.505e+04	−4.56
	^{8}Be	$^{274}112$	24.21	2.008e−35	1.502e−14	13.66
			24.65[a]	1.996e−34	1.520e−13	12.66
	^{12}C	$^{270}110$	42.97	2.809e−39	3.362e−18	17.31
			43.69[a]	5.261e−38	6.402e−17	16.03
$^{284}116$	^{4}He	$^{280}114$	11.61	5.316e−19	2.835e+02	−2.61
			11.82[a]	1.730e−18	9.389e+02	−3.13
	^{8}Be	$^{276}112$	23.12	6.286e−38	4.489e−17	16.19
			23.71[a]	1.653e−36	1.210e−15	14.75
	^{12}C	$^{272}110$	42.33	2.537e−40	2.991e−19	18.37
			42.41[a]	3.548e−40	4.190e−19	18.22
$^{286}116$	^{4}He	$^{282}114$	11.45	2.359e−19	1.240e+02	−2.25
			11.18[a]	4.640e−20	2.382e+01	1.54
	^{8}Be	$^{278}112$	21.33	1.714e−42	1.290e−21	20.79
			22.56[a]	3.025e−39	2.108e−18	17.52
	^{12}C	$^{274}110$	40.99	1.041e−42	1.188e−21	20.77
			41.05[a]	1.353e−42	1.547e−21	20.65
$^{288}116$	^{4}He	$^{284}114$	11.32	1.155e−19	6.006e+01	−1.94
			10.84[a]	6.183e−21	3.078	−0.65
$^{290}116$	^{4}He	$^{286}114$	11.31	1.734e−19	6.097e+01	−1.94
			10.58[a]	1.260e−21	0.612	0.05
			11.00[b]	1.863e−20	9.416	−1.13
$^{292}116$	^{4}He	$^{288}114$	10.71	3.145e−21	1.547	−0.35
			10.34[a]	2.76e−22	0.131	0.72
			10.80[b]	5.758e−21	2.857	−0.62

[a]Ref. [55], [b]ref. [59].

^{22}O from $^{314}116$ isotopes are also probable for emission. This stresses the role of near spherical shell closure of the daughter nuclei at $N = 184$.

We would like to point out that Gupta *et al* [47] studied the shell structure in superheavy region by calculating Q-values, barrier penetrability and preformation

Table 2. The computed half-life values, barrier penetrability and other characteristics of $^{294-314}116$ isotopes with zero angular momentum transfers. Masses are taken from [30,51].

Parent nuclei	Emitted cluster	Daughter nuclei	Q-value (MeV)	Penetrability P	Decay constant	$\log_{10} T_{1/2}$
$^{294}116$	^{4}He	$^{290}114$	10.98	1.849e−20	9.321	−1.13
			10.17[a]	9.293e−23	0.043	1.20
$^{296}116$	^{4}He	$^{292}114$	11.51	4.995e−19	2.641e+02	−2.58
			10.51[a]	9.897e−22	0.478	0.16
$^{298}116$	^{4}He	$^{294}114$	11.23	9.697e−20	5.001e+01	−1.86
			10.27[a]	2.124e−22	0.1	0.84
$^{300}116$	^{4}He	$^{296}114$	11.41	3.001e−19	1.572e+02	−2.36
			10.14[a]	9.299e−23	0.043	1.204
$^{302}116$	^{4}He	$^{298}114$	11.95	6.731e−18	3.694e+03	−3.73
			11.73[a]	1.994e−18	1.704e+03	−3.19
	^{8}Be	$^{294}112$	20.77	1.517e−43	9.730e−23	21.85
			19.75[a]	1.467e−46	8.954e−26	24.89
$^{304}116$	^{4}He	$^{300}114$	11.92	6.083e−18	3.330e+03	−3.68
			10.89[a]	1.479e−20	7.935	−1.03
	^{8}Be	$^{296}112$	21.34	6.811e−42	4.490e−21	20.19
			20.65[a]	7.942e−44	5.066e−23	22.14
$^{306}116$	^{4}He	$^{302}114$	11.46	4.858e−19	2.557e+02	−2.57
			10.13[a]	1.054e−22	0.049	1.15
	^{8}Be	$^{298}112$	20.87	3.802e−43	2.451e−22	21.45
			19.68[a]	1.166e−46	7.087e−26	24.99
$^{308}116$	^{4}He	$^{304}114$	11.02	3.744e−20	1.895e+01	−1.44
			9.37[a]	4.173e−25	0.179e−03	3.59
	^{14}C	$^{294}110$	41.26	3.975e−42	4.498e−21	20.19
$^{310}116$	^{4}He	$^{306}114$	10.41	8.023e−22	0.384	0.26
			8.42[a]	1.458e−28	5.635e−08	7.09
	^{14}C	$^{296}110$	40.36	6.380e−44	7.062e−23	21.99
$^{312}116$	^{4}He	$^{308}114$	7.81	4.246e−31	1.523e−10	9.66
			8.16[a]	1.358e−29	5.090e−09	8.13
	^{22}O	$^{290}108$	57.9	1.041e−49	1.633e−28	27.63
$^{314}116$	^{4}He	$^{310}114$	6.15	7.601e−40	2.148e−19	18.51
			7.93[a]	1.518e−30	5.527e−10	9.10

[a]Ref. [55].

probability for both alpha and heavy cluster decay. These authors studied alpha decay of $^{293}118$ and its subsequent parents ending the chain in $^{269}106$, and cluster decays of all these parents in the alpha decay chain. The calculated alpha half-life value of $^{285}114$ shows a strong peak which indicates magic shell closure at either

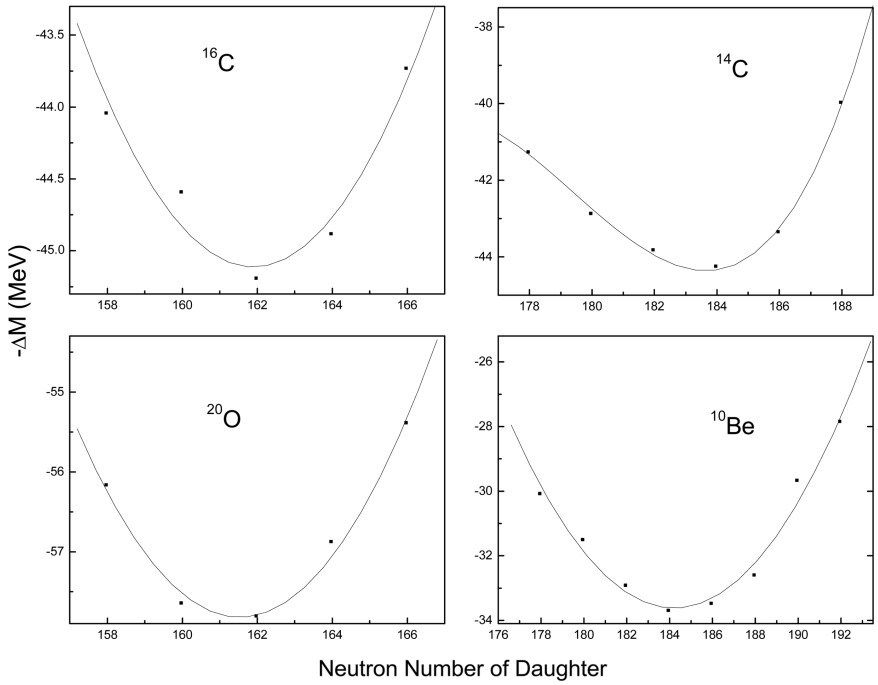

Figure 9. Mass parabola for ^{16}C, ^{14}C, ^{20}O, ^{10}Be cluster emissions from $Z = 116$ parent.

or both $Z = 114$, $N = 172$. This is supported by a small Q-value and small (deeper minima) penetrability and preformation factor (figure 3 of ref. [47]). The calculation done by these authors for various cluster decays from these parents (plot of $\log_{10} T_{1/2}$ and Q-value vs. mass number of parent, figure 4 of ref. [47]) also indicate the presence of deformed shell closure at $N = 162$ and $Z = 106$.

In the present work Q-values are calculated from experimental binding energies [30] supplemented by finite range droplet model description of Moller *et al* [48]. So the full shell effects are contained in our calculation that comes from experimental and/or calculated binding energies. The shell effects in the calculated binding energy are obtained in the Strutinsky way [49,50] by using folded Yukawa single particle potential and macroscopic finite range droplet model.

The single particle level calculations show that the shell closures in the superheavy mass region are isospin-dependent. In superheavy nuclei the spin–orbit interaction can open substantial shell gaps, e.g. between the proton $2f_{7/2}$–$2f_{5/2}$ spin–orbit partners. A nucleus with $Z = 114$ protons will fill all orbitals up to the $2f_{7/2}$ shell, and it is the strength of the spin–orbit interaction that determines the size of the $Z = 114$ gap. From single particle orbitals predicted around the Fermi surface, both the two-neutron structure $\{7/2^+[624]_\upsilon \times 1/2^+[620]_\upsilon\}^{(3+)}$ and the two-proton structure $\{1/2^-[521]_\pi \times 7/2^-[514]_\pi\}^{(3+)}$ can be formed. The $N = 184$ neutron shell closure is due to the filling up of all orbitals up to the $1j_{15/2}$ state and the size of the shell gap is related to the strength of the spin–orbit interaction

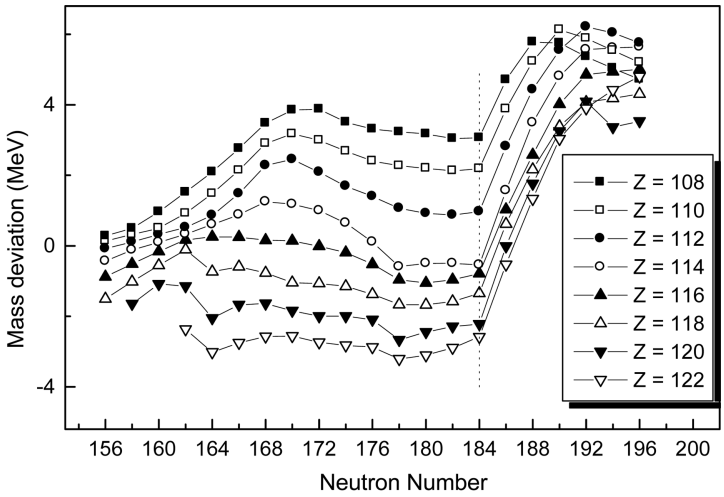

Figure 10. Plot connecting mass deviation with neutron number for various parents with $Z = 108$–122.

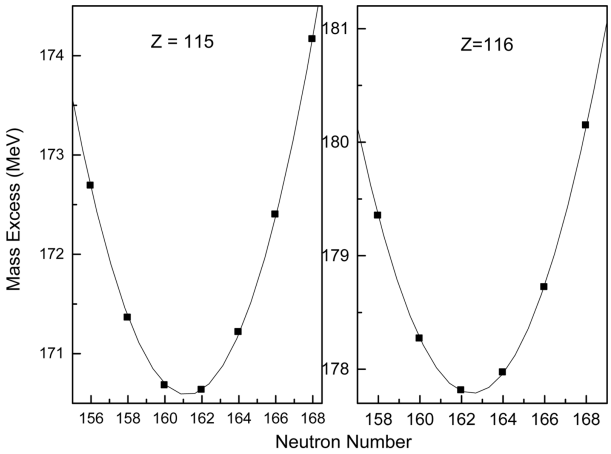

Figure 11. Isotopic mass parabola connecting mass excess with neutron number. The masses are taken from [60].

while the sub-magic shell closure at $N = 162$ is due to the filling up of all orbitals up to the $2g_{7/2}$ level.

From table 1 it is found that ^{4}He from $^{280}116$ and $^{302}116$ parents have the lowest half-life value compared to other decay modes including that of heavier clusters. This indicates the neutron magicity at 162 and 184 of daughter nuclei. In alpha and cluster radioactivity it is found that half-life has minimum value for those decays which lead to doubly magic daughter [51]. Keeping this in mind we can conclude that proton shell closure occurs at $Z = 114$ in the superheavy region. Our studies show that $^{276}_{162}114$ is deformed doubly magic and $^{298}_{184}114$ is spherical doubly magic.

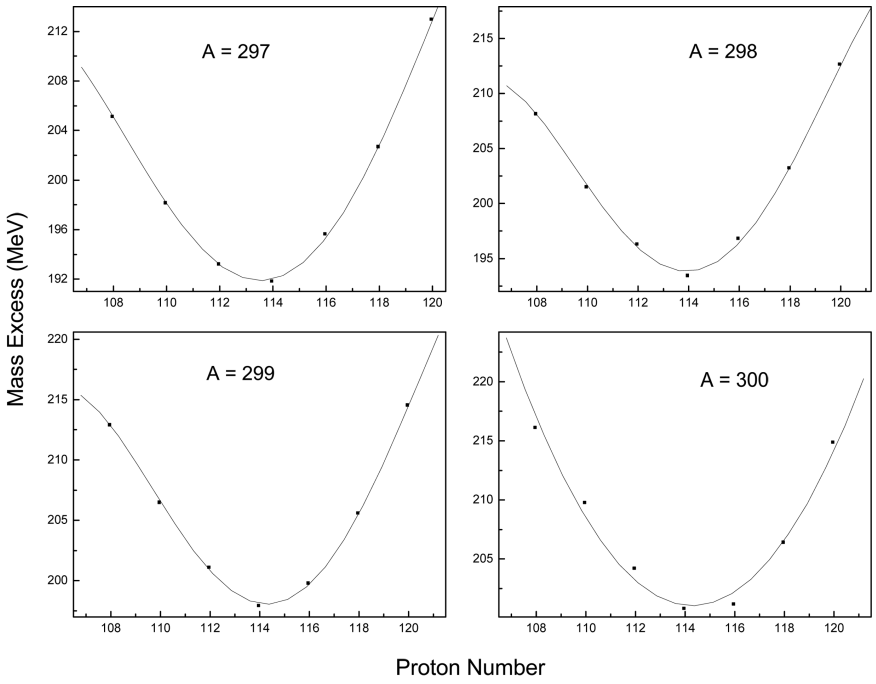

Figure 12. Isobaric mass parabola connecting mass excess with proton number. The masses are taken from [55].

On the basis of the preformed cluster model, Gupta *et al* [47] revealed that alpha decay half-life for $Z = 114$ and $A = 285$ is very high which means that the parent nucleus $^{285}114$ is very stable against alpha decay. This stability can be attributed to the magicity of proton at $Z = 114$. We would also like to point out that the finite range droplet model with folded Yukawa single particle potentials (FRDM+FY) [52] and the Yukawa plus exponential model with Wood–Saxon single particle potential (YPE+WS) [53,54] confirm the prediction of $^{298}_{184}114$ as the next spherical doubly magic nucleus.

Figure 10 represents the plot connecting mass deviation with neutron number for superheavy nuclei with $Z = 108$–122. The mass deviations are obtained by subtracting mass of an undistorted liquid drop [12] from the theoretical mass estimate of KUTY [55]. The mass deviation represents the shell correction in a method other than Strutinsky [49,50]. The mass of an undistorted liquid drop is given by

$$M_0 = M_{\mathrm{n}}N + M_{\mathrm{H}}Z - C_1A + C_2A^{2/3} + C_3\frac{Z^2}{A^{1/3}} - C_4\frac{Z^2}{A} + \delta. \qquad (17)$$

Here M_{n} is the neutron mass and M_{H} is the mass of hydrogen atom, the third term is the volume energy term, fourth term represents the surface energy, fifth term is the Coulomb energy term and the last term is the odd–even correction [56]. From these plots we see that a large deviation in mass difference occur at $N = 184$, the spherical neutron shell closure.

Following the prescription of Zeldes [57] we studied isotopic and isobaric mass parabola, the plot connecting mass excess and neutron number. Figure 11 shows isotopic mass parabola for $Z = 115$ and 116. Figure 12 represents isobaric mass parabola for $A = 297$–300. The minima (slope discontinuity) in figure 11 occur at the magic neutron number $N = 162$ and minima (slope discontinuity) in figure 12 indicate proton magicity at $Z = 114$. We would like to point out that by noting the minima in mass excess it will be possible to find neutron and proton magicities in superheavy region.

We would like to point out also that according to Gupta *et al* [58] once the fragmentation potential (driving potential) is minimized in η_Z and the behaviour of $T_{1/2}$ studied as a function of N (equivalently η_N) there is no need for plotting mass parabolas (figures 9, 11, 12) since the three variables η, η_Z and η_N are connected and only two of them are enough. But since only few atoms of short-lived superheavy nuclei are produced it will not be possible to find neutron and proton magicities in superheavy region by cluster radioactivity experiments. However, in future more mass measurements will be available and by noting the minima in mass parabola, it will be possible to find neutron and proton magicity in superheavy region.

Acknowledgement

One of the authors (KPS) would like to thank the University Grants Commission, Govt. of India for the financial support under project No. MRP(S)-352/2005 (X Plan)/KLKA 002/UGC-SWRO.

References

[1] A Sandulescu, D Poenaru and W Greiner, *Sov. J. Part. Nucl.* **II**, 528 (1980)
[2] R K Gupta, in: *Heavy elements and related new phenomena* edited by W Greiner and R K Gupta (World Scientific Pub., Singapore, 1999) Vol. **I**, p. 536
[3] H J Rose and G A Jones, *Nature (London)* **307**, 245 (1984)
[4] R Bonetti and A Guglielmetti, in: *Heavy elements and related new phenomena* edited by W Greiner and R K Gupta (World Scientific Pub., Singapore, 1999) Vol. **II**, p. 643
[5] S Kumar, M Balasubramaniam, R K Gupta, G Munzenberg and W Scheid, *J. Phys. G: Nucl. Part. Phys.* **29**, 625 (2003)
[6] S Singh, R K Gupta, W Scheid and W Greiner, *J. Phys. G: Nucl. Part. Phys.* **18**, 1243 (1992)
[7] R K Gupta, S Singh, R K Puri and W Scheid, *Phys. Rev.* **C47**, 561 (1993)
[8] R K Gupta, S Singh, G Munzenberg and W Scheid, *Phys. Rev.* **C51**, 2623 (1995)
[9] H J Fink, J A Marhun, W Scheid and W Greiner, *Z. Phys.* **268**, 321 (1974)
[10] S S Malik, S Singh, R K Puri, S Kumar and R K Gupta, *Pramana – J. Phys.* **32**, 419 (1989)
[11] D N Poenaru, D Schnabel, W Greiner, D Mazilu and R Gherghescu, *At. Data. Nucl. Data Tables* **48**, 231 (1991)
[12] W D Myers and W J Swiatecki, *Nucl. Phys.* **A81**, 1 (1966)
[13] M Bender, K Rutz, P G Reinhard, J A Maruhn and W Greiner, *Phys. Rev.* **C60**, 034304 (1999)

[14] J Decharge, J F Berger, K Dietrich and M S Weiss, *Phys. Lett.* **B451**, 275 (1999)
[15] A V Afanasjev and S Frauendorf, *Phys. Rev.* **C71**, 024308 (2005)
[16] J C Pei, F R Xu and P D Stevenson, *Phys. Rev.* **C71**, 034302 (2005)
[17] S K Patra, R K Gupta and W Greiner, *Mod. Phys. Lett.* **A12**, 1727 (1997)
[18] Yu Ts Oganessian, V K Utyonkov, Yu V Lobanov, F Sh Abdullin, A N Polyakov, I V Shirokovsky, Yu S Tsyganov, G G Gulbekian, S L Bogomolov, B N Gikal, A N Mezentsev, S Iliev, V G Subbotin, A M Sukhov, A A Voinov, G V Buklanov, K Subotic, V I Zagrebaev, M G Itkis, J B Patin, K J Moody, J F Wild, M A Stoyer, N J Stoyer, D A Shaughnessy, J M Kenneally, P A Wilk, R W Lougheed, R I Il'kaev and S P Vesnovskii, *Phys. Rev.* **C69**, 054607 (2004)
[19] Yu Ts Oganessian, V K Utyonkov, Yu V Lobanov, F Sh Abdullin, A N Polyakov, I V Shirokovsky, Yu S Tsyganov, A N Mezentsev, S lliev, V G Subbotin, A M Sukhov, O V Ivanov, A A Voinov, K Subotic, V I Zagrebaev, M G Itkis, K J Moody, J F Wild, M A Stoyer, C A Laue, D A Shaughnessy, J B Patin, R W Lougheed, *JINR Communication* D7-2002-287 Dubna (2002); *Lawrence Livermore National Laboratary Report*, UCRL-ID-151519 (2002)
[20] K P Santhosh and Antony Joseph, *Proc. Int. Natl. Symp. Nucl. Phys. (India)* **B43**, 296 (2000)
[21] K P Santhosh and Antony Joseph, *Pramana – J. Phys.* **58**, 611 (2002)
[22] K P Santhosh and Antony Joseph, *Ind. J. Pure Appl. Phys.* **42**, 806 (2004)
[23] K P Santhosh and Antony Joseph, *Pramana – J. Phys.* **62**, 957 (2004)
[24] R K Biju, Sabina Sahadevan, K P Santhosh and Antony Joseph, *Pramana – J. Phys.* **70**, 617 (2008)
[25] K P Santhosh, R K Biju and Antony Joseph, *J. Phys. G: Nucl. Part. Phys.* **35**, 085102 (2008)
[26] J Blocki, J Randrup, W J Swiatecki and C F Tsang, *Ann. Phys. (N.Y.)* **105**, 427 (1977)
[27] J Blocki and W J Swiatecki, *Ann. Phys (N.Y.)* **132**, 53 (1981)
[28] D N Poenaru, M Ivascu, A Sandulescu and W Greiner, *Phys. Rev.* **C32**, 572 (1985)
[29] K P Santhosh and Antony Joseph, *Pramana – J. Phys.* **55**, 375 (2000)
[30] G Audi and A H Wapstra, *Nucl. Phys.* **A595**, 409 (1995)
[31] D R Saroha, N Malhotra and R K Gupta, *J. Phys. G: Nucl. Part. Phys.* **11**, L27 (1985)
[32] Y J Shi and W J Swiatecki, *Nucl. Phys.* **A438**, 450 (1985)
[33] S S Malik and R K Gupta, *Phys. Rev.* **C39**, 1992 (1989)
[34] G A Lalazissis, M M Sharma, P Ring and Y K Gambhir, *Nucl. Phys.* **A608**, 202 (1996)
[35] S Cwiok, W Nazarewicz and P H Heenen, *Phys. Rev. Lett.* **83**, 1108 (1999)
[36] Y K Gambhir, A Bhagwat and M Gupta, arXiv:Nucl-th/0505067**v1** (2005)
[37] K Rutz, M Bender, T Burvenich, T Schilling, P G Reinhard, J A Maruhn and W Greiner, *Phys. Rev.* **C56**, 238 (1997)
[38] Yu Ts Oganessian, V K Utyonkov, Yu V Lobanov, F Sh Abdullin, A N Polyakov, R N Sagaidak, I V Shirokovsky, Yu S Tsyganov, A A Voinov, G G Gulbekian, S L Bogomolov, B N Gikal, A N Mezentsev, S Iliev, V G Subbotin, A M Sukhov, K Subotic, V I Zagrebaev, G K Vostokin, M G Itkis, K J Moody, J B Patin, D A Shaughnessy, M A Stoyer, N J Stoyer, P A Wilk, J M Kenneally, J H Landrum, J F Wild and R W Lougheed, *Phys. Rev.* **C74**, 044602 (2006)
[39] Yu Ts Oganessian, V K Utyonkov, Yu V Lobanov, F Sh Abdullin, A N Polyakov, I V Shirokovsky, Yu S Tsyganov, G G Gulbekian, S L Bogomolov, B N Gikal, A N Mezentsev, S Iliev, V G Subbotin, A M Sukhov, A A Voinov, G V Buklanov,

K Subotic, V I Zagrebaev, M G Itkis, J B Patin, K J Moody, J F Wild, M A Stoyer, N J Stoyer, D A Shaughnessy, J M Kenneally, P A Wilk, R W Lougheed, R I Il'kaev and S P Vesnovskii, *Phys. Rev.* **C70**, 064609 (2004)
[40] A Sobiczewski, Z Patyk and S Cwoik, *Phys. Lett.* **B224**, 1 (1989)
[41] V E Viola and G T Seaborg, *J. Inorg. Nucl. Chem.* **28**, 741 (1966)
[42] Michal Bender, arXiv:Nucl-th/9911066**v1** (1999)
[43] D N Poenaru, I H Plonski and W Greiner, *Phys. Rev.* **C74**, 014312 (2006)
[44] D N Poenaru, Y Nagame, R A Gherghescu and W Greiner, *Phys. Rev.* **C65**, 054308 (2002)
[45] H Zhang, W Zuo, J Li and G Royer, *Phys. Rev.* **C74**, 017304 (2006)
[46] O A P Tavares, E L Medeiros and M L Terranova, *J. Phys. G: Nucl. Part. Phys.* **31**, 129 (2005)
[47] R K Gupta, Sushil Kumar, Rajesh Kumar, M Balasubraminam and W Scheid, *J. Phys. G: Nucl. Part. Phys.* **28**, 2879 (2002)
[48] P Moller, J R Nix, W D Myers and W J Swiatecki, *At. Data Nucl. Data Tables* **59**, 185 (1995)
[49] V M Strutinsky, *Nucl. Phys.* **A95**, 420 (1967)
[50] V M Strutinsky, *Nucl. Phys.* **A122**, 1 (1968)
[51] R K Gupta and W Greiner, *Int. J. Mod. Phys.* **E3**, 335 (1994)
[52] P Moller, J R Nix and K L Kratz, *At. Data Nucl. Data Tables* **66**, 131 (1997)
[53] I Muntian, S Hoffmann, Z Patyk and A Sobiczewski, *Acta Phys. Pol.* **B34**, 2073 (2003)
[54] I Muntian, Z Patyk and A Sobiczewski, *Phys. At. Nucl.* **66**, 1015 (2003)
[55] H Koura, T Tachibana, M Uno and M Yamada, *Prog. Theor. Phys.* **113**, 305 (2005)
[56] A H Wapstra, in: *Handbuch der Physik* edited by F Flugge (Springer-Verlag, Berlin, 1958) Vol. 38/1, p. 1
[57] N Zeldes, in: *Handbook of nuclear properties* edited by D N Poenaru and W Greiner (Oxford Science Pub., New York, 1996) p. 12
[58] R K Gupta, W Scheid and W Greiner, *Phys. Rev. Lett.* **35**, 353 (1975)
[59] M Gupta and T W Durrows, *Nucl. Data Sheets* **106**, 251 (2005)
[60] S Liran, A Marinou and N Zeldes, arXiv:nucl-th/0102055v1 (2001)